Supplementary Information

EPAC1 activation by cAMP stabilizes CFTR at the membrane by promoting its interaction with NHERF1

Miguel J Lobo, Margarida D Amaral, Manuela Zaccolo, Carlos M Farinha

Figure S1

Figure S2

Figure S3

Figure S4

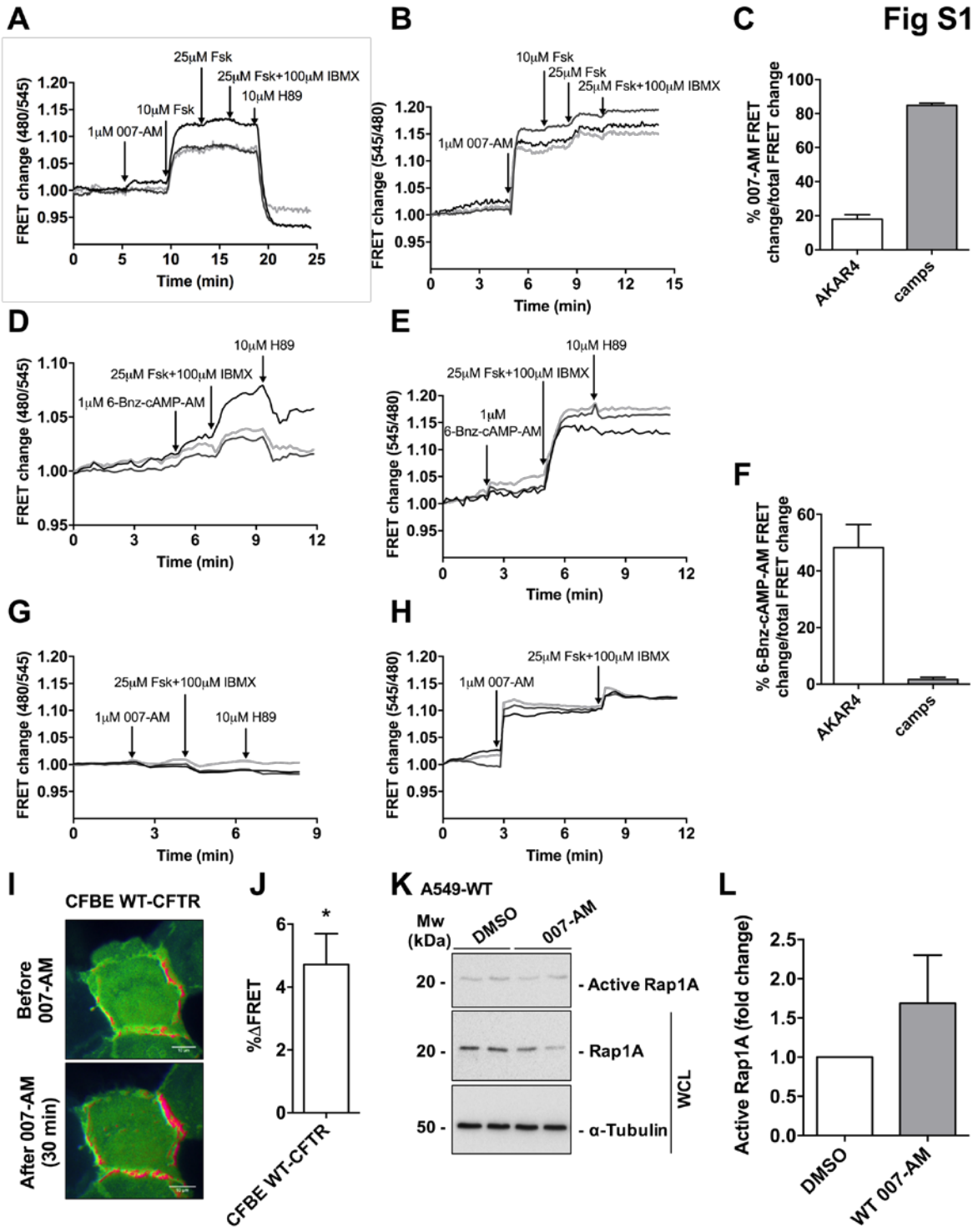
A
B
C
Fig S1
25μM Fsk
25μM Fsk+100μM IBMX
10μM H89
10μM Fsk
1μM 007-AM
FRET change (480/545)
FRET change (545/480)
Time (min)
% 007-AM FRET change/total FRET change
AKAR4
camps
D
E
F
1μM 6-Bnz-cAMP-AM
% 6-Bnz-cAMP-AM FRET change/total FRET change
G
H
I
CFBE WT-CFTR
Before 007-AM
After 007-AM (30 min)
J
%ΔFRET
CFBE WT-CFTR
K
A549-WT
Mw (kDa)
DMSO
007-AM
- Active Rap1A
- Rap1A
- α-Tubulin
WCL
L
Active Rap1A (fold change)
DMSO
WT 007-AM

Figure S1: cAMP-dependent activation of EPAC1 and PKA in CFBE cells. FRET signal from (**A**) PKA activity-sensor AKAR4 and the (**B**) cAMP-sensor based on EPAC1 (camps) upon stimulation with 1 µM 007-AM followed by increasing concentrations of Fsk. 25uM Fsk + 100uM IBMX represents a saturating condition where adenylate cyclases are fully activated and PDEs are inhibited, leading to higher levels of cAMP. H89, a PKA inhibitor, was used to show that the FRET change is due to a change in PKA activity. FRET change is the normalized 545nm/480nm or 480nm/545nm value calculated at each acquisition time point. The three lanes of each plot represent 3 different and independent cells. (**C**) Summary of all experiments performed in A and B, showing the percentage of 007-AM-induced FRET change compared to the maximum FRET change for both sensors. Data represent mean ± SEM. n = 30/19 cells, 9/6 experiments (AKAR4/camps). FRET signal from (**D**) AKAR4 and (**E**) camps upon stimulation with 1 µM 6-Bnz-cAMP-AM followed by 25uM Fsk + 100uM IBMX and then 10uM H89. The three lanes of each plot represent 3 different and independent cells. (**F**) Summary of all experiments performed in D and E, showing the percentage of 6-Bnz-cAMP-AM-induced FRET change compared to the maximum FRET change for both sensors. Data represent mean ± SEM. n = 11/18 cells, 5/5 experiments (AKAR4/camps). FRET signal from (**G**) AKAR4 and (**H**) camps upon stimulation with 1 µM 007-AM followed by 25uM Fsk + 100uM IBMX. The three lanes of each plot represent 3 different and independent cells. (**I**) EPAC1 activation after treatment with 007-AM. Analysis of Raichu-Rap FRET sensor upon stimulation of CFBE cells expressing wt-CFTR with 1µM 007-AM. Intensity-modulated pseudo-color images are shown here. Images show FRET signal before (upper panel) and 30 min after addition of 1µM 007-AM (lower panel). Scale bars, 10 µm. (**J**) %ΔFRET represents the fold increase of the FRET signal at the PM (as a percentage) 30 min after the addition of 007-AM relative to pre-stimulus levels. * means that the FRET signal after addition of 007-AM is significantly different compared to pre-stimulus condition ($p<0.05$). Data represent mean ±

SEM. n = 28 cells, 13 experiments. (**K**) Western Blot showing the effect of 007-AM treatment upon the fraction of active Rap1A (using a specific pull-down assay – see Materials and Methods), in A549 cells expressing wt-CFTR. Cells were incubated with 1µM 007-AM for 2h (or DMSO as control). (**L**) Fold increase of active Rap1A after treatment with 007-AM for A549 cells expressing wt-CFTR. Amount of active Rap1A was normalized to the amount of total Rap1A and shown as fold change relatively to DMSO incubated cells. Data represent mean ± SEM (n=4).

Fig S2

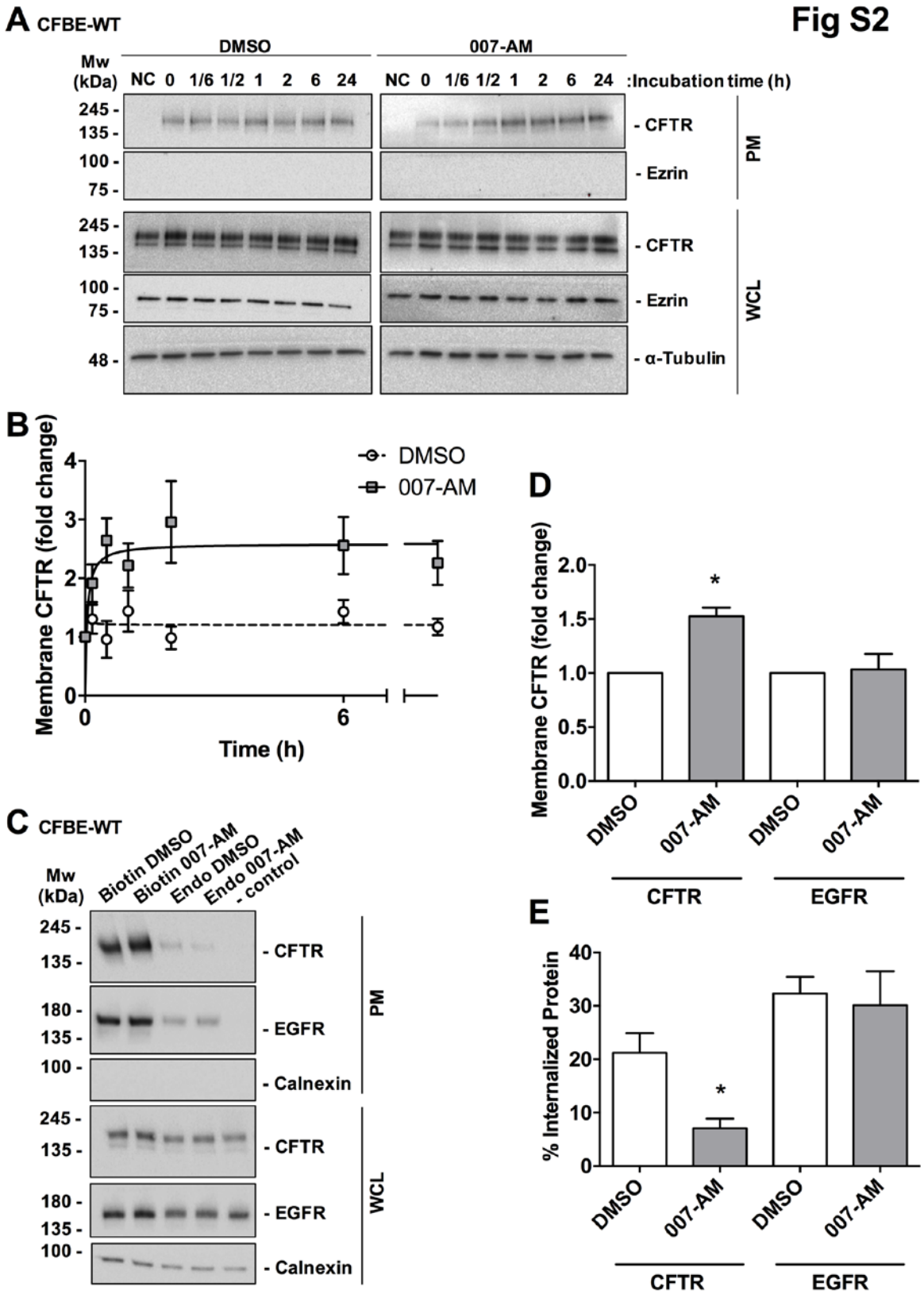
A CFBE-WT
DMSO
007-AM
Mw (kDa)
NC 0 1/6 1/2 1 2 6 24
NC 0 1/6 1/2 1 2 6 24
:Incubation time (h)
245 -
135 -
100 -
75 -
48 -
- CFTR
- Ezrin
- α-Tubulin
PM
WCL
B
Membrane CFTR (fold change)
DMSO
007-AM
Time (h)
C CFBE-WT
Biotin DMSO
Biotin 007-AM
Endo DMSO
Endo 007-AM
- control
180 -
- EGFR
- Calnexin
D
E
% Internalized Protein
CFTR
EGFR

Figure S2: CFTR and EGFR surface expression and endocytosis under EPAC1 activation. (**A**) Time-course of CFTR plasma membrane levels under EPAC1 activation with 007-AM. CFBE-wt cells were treated with 1 µM 007-AM for different time periods. After cell surface biotinylation and streptavidin pull-down, CFTR levels were assessed by WB. Samples not treated with biotin were considered as a negative control (NC). (**B**) Quantification of the amount of CFTR at the PM. Amount of CFTR at the PM was normalized to the amount of total CFTR and shown as fold change relatively to 0h. Data represent mean ± SEM. n=3/4. (**C**) CFBE cells expressing wt-CFTR treated with 1µM 007-AM for 2h (or DMSO as control) were subjected to cell surface biotinylation, followed by incubation at 37ºC (for 10 minutes). After that, cells were treated with a GSH solution and, after cell lysis and streptavidin pull-down, CFTR and EGFR were detected by WB. Samples not treated with GSH were considered as a positive control (Biotin). Samples not incubated at 37ºC were considered as a negative control. (**D**) Quantification of the amount of CFTR/EGFR at the PM. Amount of CFTR/EGFR at the PM was normalized to the amount of total CFTR/EGFR and shown as fold change relatively to DMSO. Data represent mean ± SEM (n=5-9). (**E**) Quantification of internalized CFTR/EGFR. The negative (-) control was subtracted from the amount of endocytosed CFTR/EGFR and values were normalized to the positive control (Biotin). Data represent mean ± SEM (n=5-7).

Fig S3

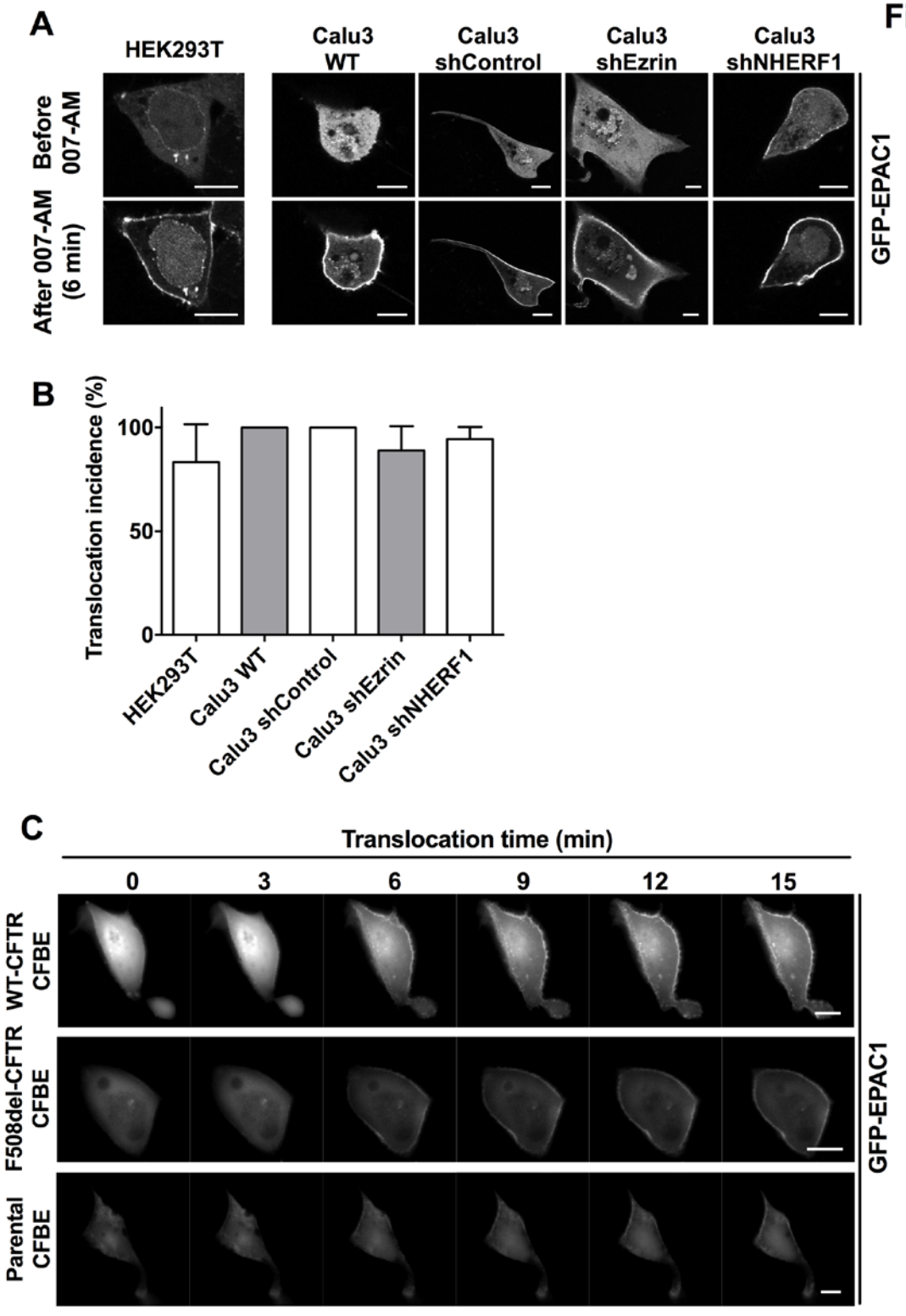
A
HEK293T
Calu3 WT
Calu3 shControl
Calu3 shEzrin
Calu3 shNHERF1
Before 007-AM
After 007-AM (6 min)
GFP-EPAC1
B
Translocation incidence (%)
100
50
0
HEK293T
Calu3 WT
Calu3 shControl
Calu3 shEzrin
Calu3 shNHERF1
C
Translocation time (min)
0
3
6
9
12
15
WT-CFTR CFBE
F508del-CFTR CFBE
Parental CFBE
GFP-EPAC1

Figure S3: EPAC1 localization in HEK293, Calu3 and CFBE cells. (**A**) Confocal live cell imaging analysis of GFP-EPAC1 localization in HEK293 and Calu3 cells. Images show EPAC1 staining before (upper panel) and 6 min after addition of 1µM 007-AM (lower panel). Scale bar 10 µm. (**B**) The bar graph shows the percentage of cells showing translocation of EPAC1 to the PM upon 007-AM stimulation (Consonni et al., 2012) (n=9-19 cells, 6-11 experiments). (**C**) Live cell imaging of GFP-EPAC1 localization in CFBE parental, CFBE-wt and CFBE-F508del cells. Images were acquired every 3 min with 1µM 007-AM added after the acquisition at minute 3. Scale bar 10 µm.

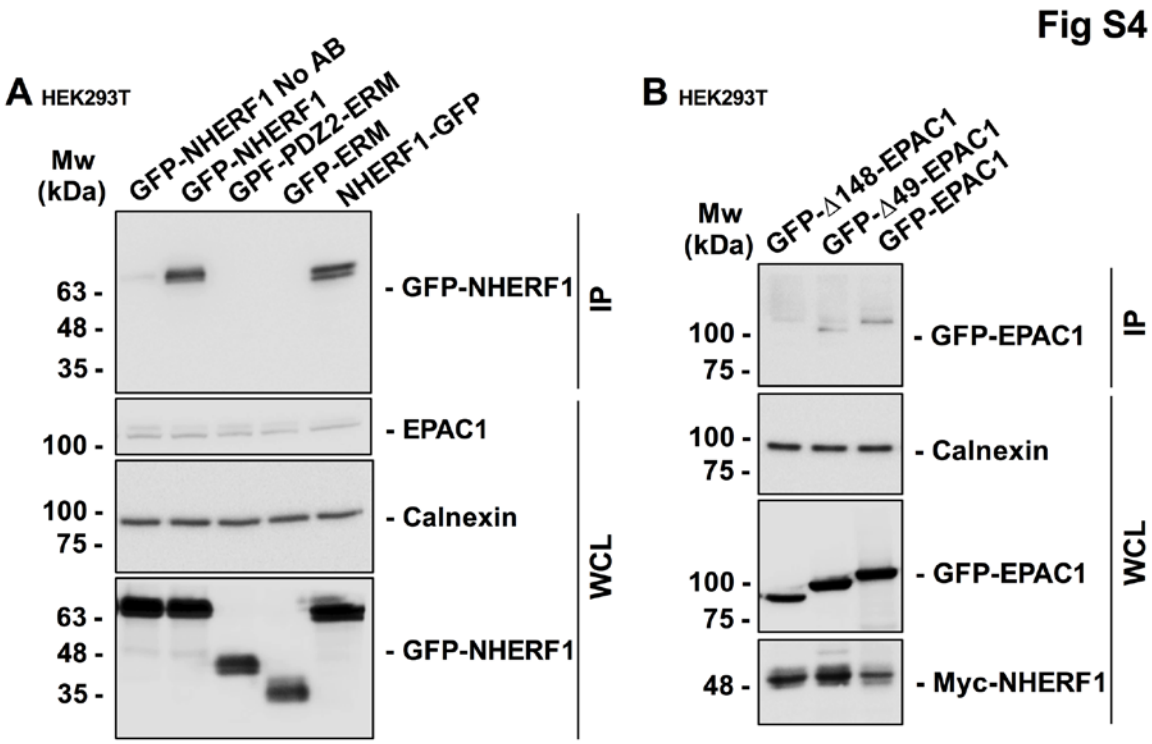

Figure S4: Model for CFTR-EPAC1 interaction. (**A**) Interaction of EPAC1 and NHERF1. Detection of NHERF1 deletion variants after immunoprecipitation of endogenously expressed EPAC1 in transiently transfected HEK293 cells. Pull-down with beads only (without conjugated antibody) was used as a negative control. GFP-NHERF1 and NHERF1-GFP have the GFP tag on either the N- or the C-terminus, respectively. GFP-PDZ2-ERM construct lacks PDZ1 domain while GFP-ERM construct lacks both PDZ1 and 2 domains. (**B**) Detection of EPAC1 deletion variants after immunoprecipitation of myc-NHERF1 in transiently transfected HEK293 cells. GFP-Δ49-EPAC1 and GFP-Δ148-EPAC1 lack the first 49 or 148 amino acids, respectively, of their N-terminal region.